JOTCS B
Journal of the Turkish Chemical Society
Section: B
Chemical Engineering
TURKISH CHEMICAL SOCIETY

Synthesis and Characterization of Cu/KIT-6 Silicas for Use in CO_2 Adsorption

Gamze GÜNDÜZ MERİÇ

Engineering Faculty, Chemical Engineering Department, Bilecik Seyh Edebali University 11210 Gulumbe Bilecik/TURKEY

Abstract: KIT-6 is a mesoporous material with cubic la3d symmetry, adjustable porous 3-dimensional (3D) silica structure, advanced wall thickness, and excellent thermal/hydrothermal stability. KIT-6, with its cubic la3d symmetrical structure, has adjustable pore size. In this study, characterization studies of Cu/KIT-6 material by preparing different Si/Cu: blank, 1, 3, 5 molar ratios were performed by SEM, SEM-Mapping, TEM, XRD, N_2 adsorption-desorption, FTIR analysis. Cu-based la3d mesoporous silica KIT-6 was synthesized by hydrothermal method and different silicon to copper (Cu) ratios $n_{Si/Cu}$: 1, 3, 5, and blank KIT-6 were investigated for CO_2 adsorption capacity at ambient conditions. The highest CO_2 adsorption of 1.70 mmol CO_2/g at 0 °C and 1.2 bar was achieved for $n_{Si/Cu}$:1 ratio Cu/KIT-6. These materials are thought to be useful for the emission of CO_2 that causes global warming.

Keywords: KIT-6, silicas, mesoporous, Cu, CO_2 capture, global warming.

Submitted: February 15, 2022. **Accepted:** May 11, 2022.

Cite this: Gündüz Meriç G. Synthesis and Characterization of Cu/KIT-6 Silicas for Use in CO2 Adsorption. JOTCSB. 2022;5(1):21–8.

***Corresponding author. E-mail:** gamze.gunduz@bilecik.edu.tr. Tel: +90228 214 1765 Fax:+90228 214 1222

INTRODUCTION

The greenhouse gases contain CH_4, CO_2, N_2O, sulfur hexafluoride, and chloro-fluorocarbons (1). CO_2 is the most serious one for global warming compared to other gases (2, 3). CO_2 concentration in the atmosphere increases rapidly and affects global warming (4). Global warming is one of the major problems to an ecosystem in the world. This rapid increase also affects the environment (5-7). CO_2 concentration will reach 450 ppm in the future (8) and it causes an increase in global surface temperature (about 2 °C) (9). For controlling global warming, CO_2 capture is the main solution according to the United Nations countries (10). CO_2 capture and storage is very important to minimize its negative effects on climate change and to reduce CO_2 emission (11, 12). Solid porous adsorbents are widely used due to their large surface area and pore volume for CO_2 adsorption techniques (13). Sun et al. (14) prepared CaO-based sorbents and they found a high-temperature CO_2 capacity of 7.6 mmol/g at 377 K and they showed excellent stability over 10 cycles. Kishor et al. (15) reported 1.56 mmol CO_2/g at 30 °C for APTES-grafted KIT-6. Huang et al. (16) studied MCM-48 for CO_2 adsorption and found 98.2 mg/g at 1 atm and room temperature. Gargiulo et al. (17) measured the highest CO_2 capacity of 5.3 mol/kg at 298 K under 1 bar with NaX RHA zeolite. Yan et al. (18) prepared zeolite NaX@NaA core-shell microspheres for its high CO_2 adsorption capacity and they reported 5.60 mmol/g CO_2 at 298 K and 100 kPa total pressure. Huang et al. (19) found that 2.2 mmol CO_2/g with amine-based MCM-48 under 1 atm at 298 K. Liu et al. (20,21) studied with N-(2-aminoethyl)-3-aminopropyltrimethoxysilane-based SBA-15 and the adsorption capacity was 0.727 mmol/g under 101.325 kPa at 333 K. Hiyoshi et al. (22) prepared aminosilanes on SBA-15 adsorbents and they reported 1.8 mmol/g- adsorbent under 15 kPa at 333 K. Zhao et al. (23) studied with porous SiO_2 supported CaO and they found a 7.5 mmol CO_2/g capacity.

KIT-6 is a mesoporous SiO_2 with a la3d structure and larger pore diameter. Most researchers in recent years have paid attention to their favorable physicochemical properties that increase the metal distribution and subsequently the accessibility of the reactants (24-28). Its specific (3D) cubic channels

give it a more suitable structure for the diffusion of reactant gas (29-31). KIT-6 is a highly stable silica framework as CO_2 support (32). On the other hand, there is very little literature working on the CO_2 adsorption capacity in silica KIT-6 supplement and there are no reports on Cu-based KIT-6. SiO_2 is also a widely available sinter-resistant and cost-effective material for economical CO_2 capture. The adsorption capacity of Cu/KIT-6 was investigated by CO_2 adsorption tests and materials were characterized by BET (Brauner-Emmett-Teller) isotherms, SEM (Scanning electron microscopy), SEM-EDX (Scanning electron microscopy, energy dispersive x-ray analysis), SEM-Mapping (Analytical mapping), TEM (Transmission electron microscopy), XRD (X-ray diffraction analysis), and FT-IR (Fourier transform infrared spectroscopy) analysis.

EXPERIMENTAL SECTION

Synthesis of mesoporous silicas

Cu-based KIT-6 with different Cu contents was prepared with a typical procedure (33). Cu/KIT-6 mesoporous la3d materials containing $n_{Si/Cu}$= 1, 3, 5 and blank KIT-6 were synthesized using Pluronic P123 (Poly(ethylene glycol)-block-poly(propyleneglycol)-block-poly(ethylene glycol)-PEG-PPG-PEG (CAS no: 9003-11-6) (Carbosynth) and n-butanol ($CH_3(CH_2)_3OH$) (CAS no: 71-36-3) (Merck). 5.0 g of P123 was dissolved in 161 mL of 0.5 M Hydrochloric acid (HCl) (38%) (Cas no: 7647-01-0) (Merck) at 35°C. After dissolution was complete, 5.0 g of n-butanol was added and the resulting mixture was stirred at 35 °C for 1 hour. In order to obtain the desired Si/Cu: 1, 3, 5 molar ratio, the metal source Copper(II) chloride ($CuCl_2$) (CAS no: 7447-39-4) (Sigma-Aldrich) and the required amount of tetraethyl orthosilicate ($Si(OC_2H_5)_4$) (CAS no: 78-10-4) (TEOS) (ABCR) were added to the mixture and it was stirred for 24 hours. The reaction mixture was taken into a 250-mL Teflon autoclave for hydrothermal treatment (24 hours at 100 °C). The resulting solid was separated and dried at 100 °C overnight. The surfactant was removed by calcination in dry air at 550 °C for 5 hours.

Material characterization

The morphology of Cu-based materials was evaluated by TEM using JEOL JEM-1220 and by SEM using the Quanta 400F Field Emission device. Textural parameters (BET surface areas, total pore volume, and pore sizes) were obtained by N_2 ads.-des. isotherms. The specific surface areas of the materials were determined by the BET method at 77 K under N_2 gas adsorption. From the plot of relative pressure (P/P_0 between 0 and 1.0) versus quantity adsorbed (cm^3 /g STP) were determined. XRD patterns of the materials were obtained with a Panalytical Empyrean device at 200 kV and 50 mA with 2Θ values ranging from 5-80° and a speed of 10°/min. Prior to measurements, materials were gassed overnight at 250 °C and 100 mmHg. ATR-FT-IR spectra were obtained on a Cary 630 between 4000 and 400 cm^{-1} using diluted samples. CO_2 adsorption was measured with a Micromeritics ASAP 2020 Analyzer at 0 °C and 1.2 bar, after which the measurement materials were degassed at 150 °C for 5 hours.

RESULTS AND DISCUSSION

The surface morphologies of the blank and Cu-based KIT-6 adsorbents were investigated with scanning electron microscopy (Figure 1). SEM-EDX analysis was also studied to determine the chemical composition of Cu/KIT-6 (Figure 2). SEM mapping analyses of the adsorbents are shown in Figure 3.

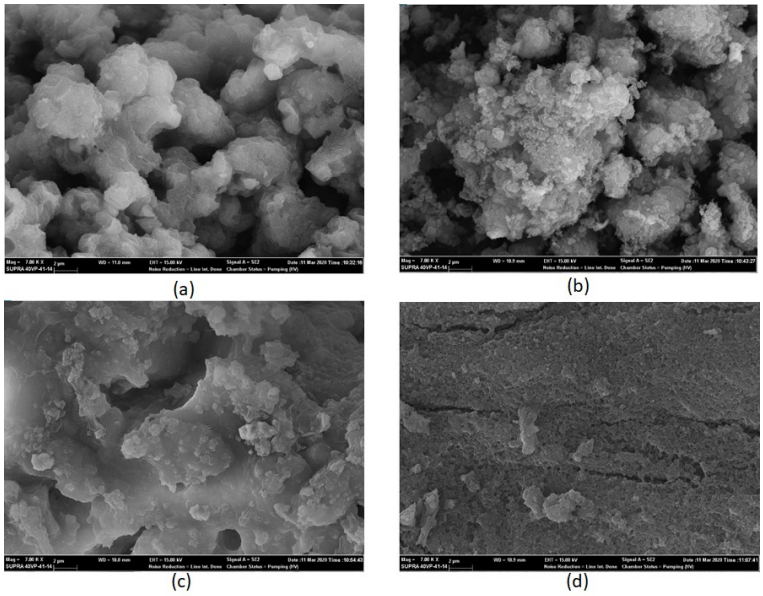

Figure 1: SEM images of (a) blank (b) 1 (c) 3 (d) 5 Si/Cu KIT-6 materials (15 kV, 7 KX).

The morphology of KIT-6 shows angular particles with a relatively flat surface (25). The sponge-like porous nature of KIT-6 was transformed to a rougher surface with the loading of Cu to silica KIT-6 support. The rock-like morphology is visible and Cu on the surface affects the surface smoothness of the materials.

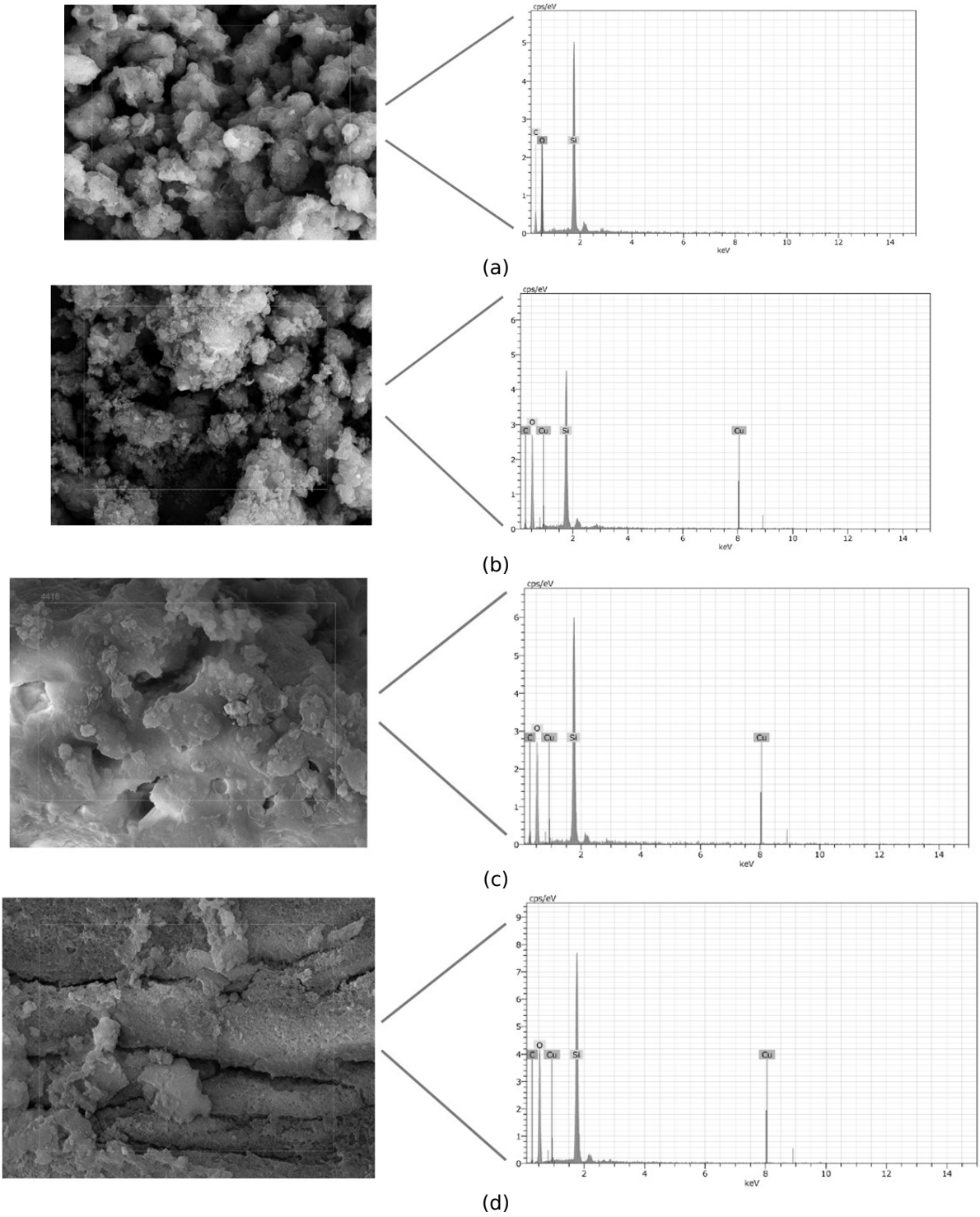

Figure 2: EDX spectra of (a) blank, (b) 1 Si/Cu, (c) 3 Si/Cu, (d) 5 Si/Cu KIT-6 materials.

The EDX analysis of Si/Cu:1, 3, 5 KIT-6 demonstrated the presence of 2.53 wt%, 1.32 wt%, and 0.34 wt% Cu, respectively in the KIT-6 framework, indicating copper was successfully incorporated into the KIT-6. EDX analysis confirms the successful synthesis of a decrease in Cu content for the Si/Cu:1, 3, 5 KIT-6, respectively because of the increase of Si content on the support KIT-6. The elemental distribution of Cu is shown in Figure 3 using SEM mapping. They were

homogeneously dispersed on the adsorbents' surface.

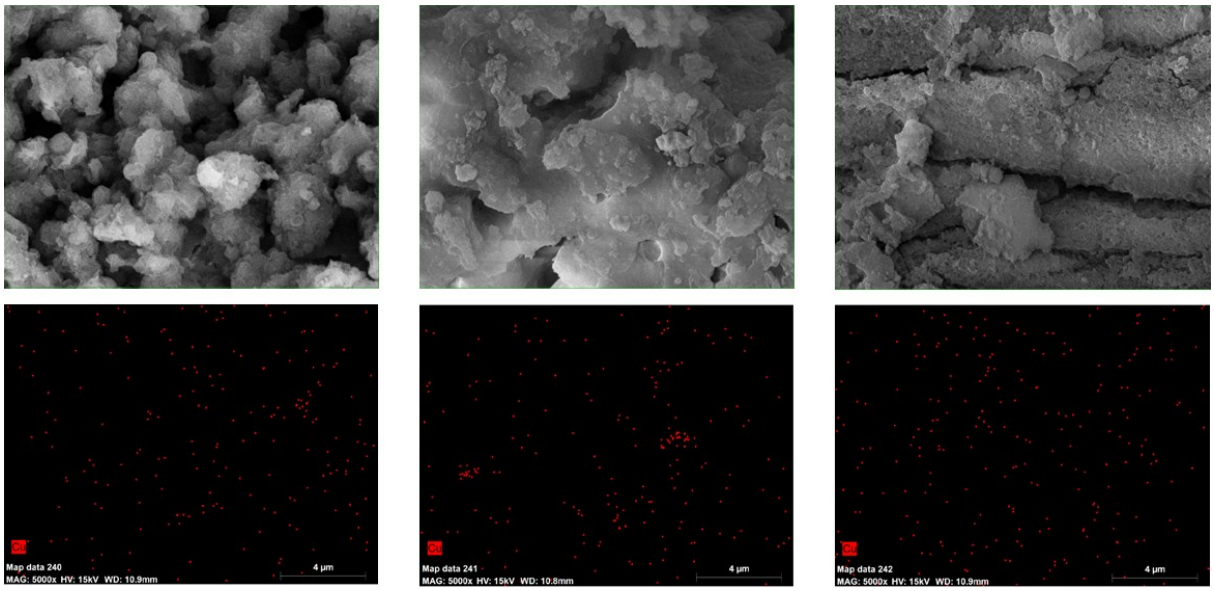

Figure 3: SEM mapping of 1 Si/Cu (left), 3 Si/Cu (middle), 5 Si/Cu (right) KIT-6 materials.

The in-site morphologies of KIT-6 materials were also investigated by TEM analysis. TEM was used to observe the internal mesoporous structure as shown in Figure 4.

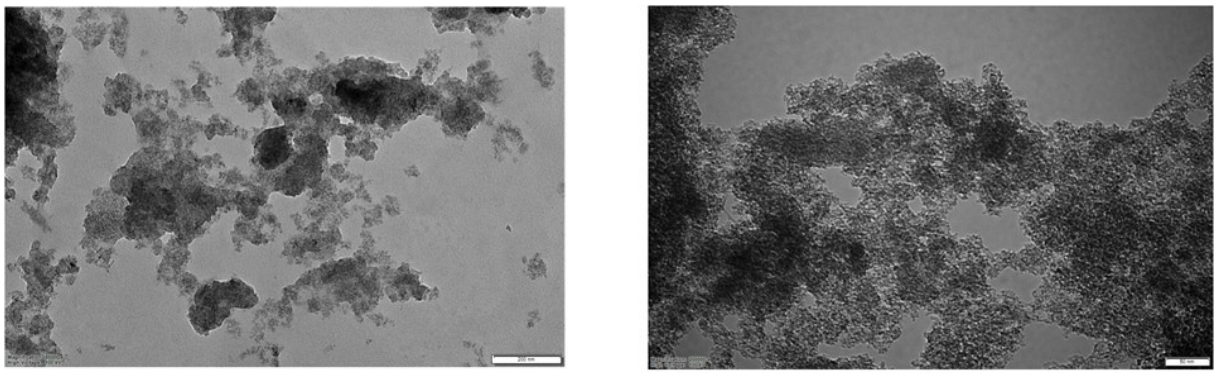

(a) (b)

Figure 4:TEM images of (a) 5 (100 kV, 80000 X) and (b) 1 Si/Cu KIT-6 (100 kV, 200000 X) materials.

The textural properties of different Cu-based and blank KIT-6 materials, such as specific surface area (S_{BET}), pore volume (V_{total}), and pore diameter, are summarized in Table 1. The mesoporous nature of KIT-6 materials was investigated using N_2 sorption analysis. The N_2 sorption isotherms for the adsorbents are shown in Figure 5. The blank KIT-6 support exhibits the characteristic type IV isotherm via the IUPAC classification with an average pore size of 4.5 nm. The isotherms of the Cu-based KIT-6 adsorbents exhibit either type II-IV with average pore sizes between 4.7-5.5 nm with hysteresis to higher relative pressure (26). N_2 adsorption-desorption isotherms of materials indicated the formation of mesoporous structure with narrow pore size distribution. The observation implies that Si/Cu:5 KIT-6 has large pores than Si/Cu:1 and Si/Cu:3 KIT-6 adsorbents (Table 1). Si/Cu:5 KIT-6 has the lowest surface area, the increase in surface area with increasing Cu loading on the support due to the porous nature of copper. The increase of porosity from copper was due to an increase in surface area and pore volume.

Table 1: Textural properties of KIT-6 materials.

Materials	BET surface area (m^2/g)	Pore volume (cm^3/g)	Pore size (nm)
KIT-6	738.72	0.618	4.5
Si/Cu:5 KIT-6	742.88	0.734	5.5
Si/Cu:3 KIT-6	763.77	0.838	4.9
Si/Cu:1 KIT-6	780.37	1.007	4.7

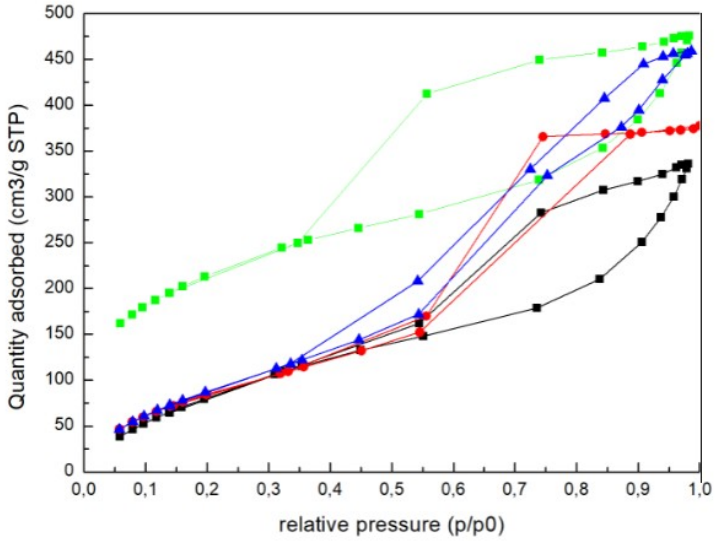

Figure 5: N_2 ads.-des. isotherms of materials (green: KIT-6, black: Si/Cu: 5 KIT-6, red: Si/Cu:3 KIT-6, blue:Si/Cu:1 KIT-6).

The crystalline phases of KIT-6 adsorbents are characterized by powder wide-angle XRD and the results are presented in Figure 6. The peaks observed at 2Θ values of 43.3, 50.4, 74, 89.8 corresponded to cubic Cu metal; 36.8, 42.8, 53.1, 66, 74.5 corresponded to cubic Cu_2O, and 32.7, 35.6, 38, 51.6, 68, 72.2 corresponded to CuO. The broad peak obtained at 23.5° corresponds to amorphous silica. The intensity of Si/Cu:1 KIT-6 was higher than the other KIT-6 materials. As the amount of Cu loaded on the structure increased, the intensity of the peaks increased as well.

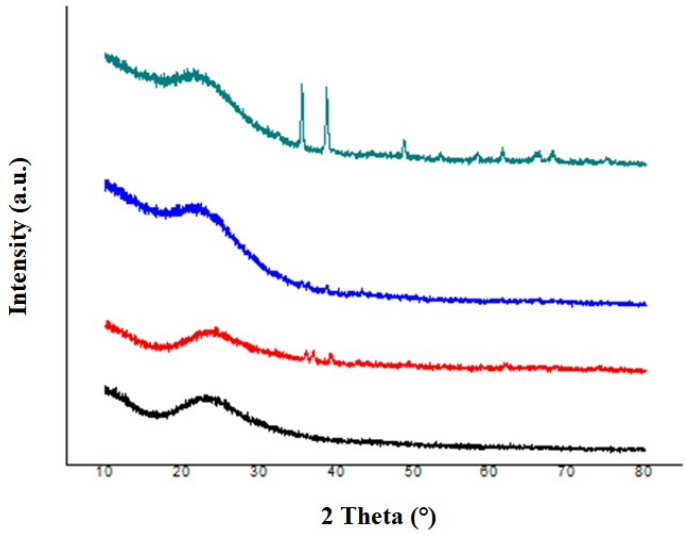

Figure 6: XRD patterns of materials (black: KIT-6, red: Si/Cu:5 KIT-6, blue: Si/Cu:3 KIT-6, green: Si/Cu:1 KIT-6).

The structural properties of KIT-6 materials were measured between 4000-400 cm^{-1} with FT-IR (Figure 7). The characteristic peak of the Si-O-Si bond appeared at about 1074 cm^{-1} for all samples due to

symmetrical stretching vibrations. The peaks at 455 cm^{-1} and 806 cm^{-1} correspond to the bending of the Si-O bond and the asymmetrical bending of the Si-O-Si bond, respectively. Symmetric stretching of Si-OH was observed around 952 cm^{-1}. Besides the band at about 3392 cm^{-1}, the peaks around 1645-1650 cm^{-1} show –OH stretching vibrations related to adsorbed water molecules that readily allow surface modification (25, 31).

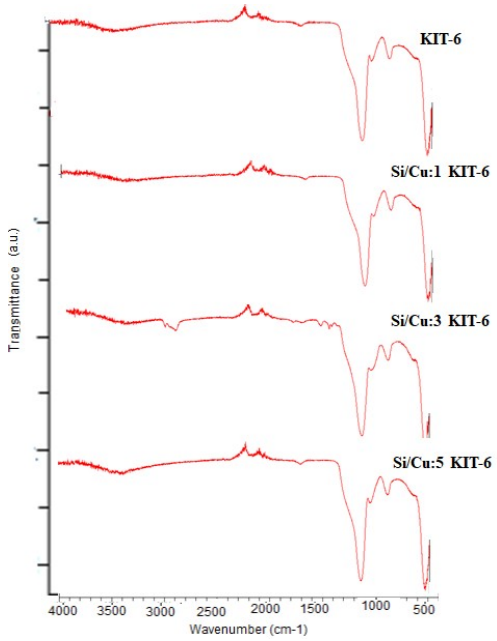

Figure 7: FT-IR spectra of KIT-6 materials.

All samples were used as adsorbents for CO_2 adsorption at 273 K and pressure up to 1.2 bar. The CO_2 adsorption capacities for the materials are shown in Figure 8. It is preferred at a lower temperature due to the CO_2 exothermic process. Among the four samples, Si/Cu:1 KIT-6 recorded the highest CO_2 adsorption with 1.70 mmol/g at 0 °C and 1.2 bar. Si/Cu:1 has the highest adsorption capacity of KIT-6 due to the Cu particles inside the porous channels and this provides adsorption sites for CO_2 molecules. As seen from the results, the amount of Cu in the KIT-6 support is the critical point for CO_2 adsorption, and the material with highest surface area is the best adsorbent. The CO_2 adsorption capacity shows a similar trend with Si/Cu:1 KIT-6 compared to other KIT-6 adsorbents (Table 2). The importance of KIT-6 mesoporosity also supports the high adsorption of CO_2 molecules. A comparison of the CO_2 capture capacities of adsorbents similar to this study is shown in Table 3. The surface area and CO_2 adsorption capacities of KIT-6 are quite high under similar pressure and temperature conditions.

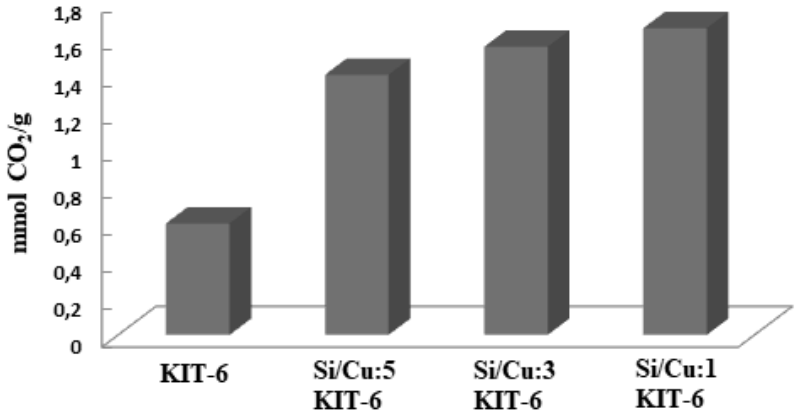

Figure 8: CO_2 capture of KIT-6 silicas (1.2 bar and 0 °C with dry CO_2 gas).

Table 2: CO_2 capture capacity of KIT-6 silicas.

Sample	CO_2 adsorbed (mmol/g)
KIT-6	0.60
Si/Cu:5 KIT-6	1.40
Si/Cu:3 KIT-6	1.55
Si/Cu:1 KIT-6	1.70

From the table of comparison of the different materials (Table 3), low temperature and pressure with a high surface area favor higher CO_2 adsorption capacity. A certain amount of added copper plays a critical role in controlling the total adsorption capacity of the KIT-6 support. It has been determined that adding a small amount of Cu to the KIT-6 structure shows a good effect on CO_2 adsorption. All literature studies also show the importance of the main properties and parameters that can be used for the CO_2 capacities of materials.

Table 3: Comparison of the different materials for CO_2 capture capacities.

Material	Temp. (°C)	Pressure (bar)	Surface area (m^2/g)	CO_2capture (mmol/g)	Ref.
An-KIT-6	30	1.00	297	0.90	(15)
Amine-MCM-41	0	1.20	279	0.83	(27)
HMS-F MS	25	1.00	636	1.00	(28)
CS-1.5	0	0.15	1187	1.25	(29)
Amine-MCM-41	30	1.20	1759	1.15	(30)
Amine-SBA-15	25	1.00	1177	1.20	(31)
Amine-KIT-6	0	1.20	1070	0.60	(32)
Cu/Si:1 KIT-6	0	1.20	780	1.70	This work
Cu/Si:5 KIT-6	0	1.20	742	1.40	This work

CONCLUSION

In this study, different amounts of Cu-loaded KIT-6 were prepared and investigated for high CO_2 capture capacity at 0 °C and 1.2 bar. The highest CO_2 adsorbed of 1.70 mmol/g was achieved at Si/Cu:1 KIT-6. It was seen that the materials with optimized Cu content on KIT-6 support showed excellent textural properties and high CO_2 adsorption capacity for the determined temperature and pressure. The adsorption capacities at 0 °C provide strong evidence at low temperature and pressure and due to the mesoporous nature of the materials, CO_2 was used as a probe molecule for investigating the porosity. The Cu-based KIT-6 combination could be used as an effective material for CO_2 capture.

REFERENCES

1. Zhou K, Chaemchuen S, Verpoort F. Alternative materials in technologies for Biogas upgrading via CO2 capture. Renewable and Sustainable Energy Reviews. 2017 Nov;79:1414–41. <DOI>.

2. Lakhi KS, Cha WS, Joseph S, Wood BJ, Aldeyab SS, Lawrence G, et al. Cage type mesoporous carbon nitride with large mesopores for CO2 capture. Catalysis Today. 2015 Apr;243:209–17. <DOI>.

3. Mutyala S, Jonnalagadda M, Mitta H, Gundeboyina R. CO2 capture and adsorption kinetic study of amine-modified MIL-101 (Cr). Chemical Engineering Research and Design. 2019 Mar;143:241–8. <DOI>.

4. Han Y, Hwang G, Kim H, Haznedaroglu BZ, Lee B. Amine-impregnated millimeter-sized spherical silica foams with hierarchical mesoporous–macroporous structure for CO2 capture. Chemical Engineering Journal. 2015 Jan;259:653–62. <DOI>.

5. Yıldız MG, Davran-Candan T, Günay ME, Yıldırım R. CO2 capture over amine-functionalized MCM-41 and SBA-15: Exploratory analysis and decision tree classification of past data. Journal of CO2 Utilization. 2019 May;31:27–42. <DOI>.

6. Gaikwad S, Kim SJ, Han S. CO2 capture using amine-functionalized bimetallic MIL-101 MOFs and their stability on exposure to humid air and acid gases. Microporous and Mesoporous Materials. 2019 Mar;277:253–60. <DOI>.

7. Zhang G, Zhao P, Xu Y. Development of amine-functionalized hierarchically porous silica for CO2 capture. Journal of Industrial and Engineering Chemistry. 2017 Oct;54:59–68. <DOI>.

8. Liu Y, Shi J, Chen J, Ye Q, Pan H, Shao Z, et al. Dynamic performance of CO2 adsorption with tetraethylenepentamine-loaded KIT-6. Microporous and Mesoporous Materials. 2010 Oct;134(1–3):16–21. <DOI>.

9. Peirce S, Russo ME, Perfetto R, Capasso C, Rossi M, Fernandez-Lafuente R, et al. Kinetic characterization of carbonic anhydrase immobilized on magnetic nanoparticles as biocatalyst for CO2 capture. Biochemical Engineering Journal. 2018 Oct;138:1–11. <DOI>.

10. Hussain M, Akhter P, Saracco G, Russo N. Nanostructured TiO2/KIT-6 catalysts for improved photocatalytic reduction of CO2 to tunable energy products. Applied Catalysis B: Environmental. 2015 Jul;170–171:53–65. <DOI>.

11. Hu L, Liu J, Zhu L, Hou X, Huang L, Lin H, et al. Highly permeable mixed matrix materials comprising ZIF-8 nanoparticles in rubbery amorphous poly(ethylene oxide) for CO2 capture. Separation and Purification Technology. 2018 Oct;205:58–65. <DOI>.

12. Wang X, Zhou J, Xing W, Liu B, Zhang J, Lin H, et al. Resorcinol–formaldehyde resin-based porous carbon spheres with high CO2 capture capacities. Journal of Energy Chemistry. 2017 Sep;26(5):1007–13. <DOI>.

13. Sari Yilmaz M. Synthesis of novel amine modified hollow mesoporous silica@Mg-Al layered double hydroxide composite and its application in CO2 adsorption. Microporous and Mesoporous Materials. 2017 Jun;245:109–17. <DOI>.

14. Sun H, Parlett CMA, Isaacs MA, Liu X, Adwek G, Wang J, et al. Development of Ca/KIT-6 adsorbents for high temperature CO2 capture. Fuel. 2019 Jan;235:1070–6. <DOI>.

15. Kishor R, Ghoshal AK. APTES grafted ordered mesoporous silica KIT-6 for CO2 adsorption. Chemical Engineering Journal. 2015 Feb;262:882–90. <DOI>.

16. Huang X, Ding J, Zhong Q. Catalytic decomposition of H2O2 over Fe-based catalysts for simultaneous removal of NOX and SO2. Applied Surface Science. 2015 Jan;326:66–72. <DOI>.

17. Gargiulo N, Pepe F, Caputo D. CO₂ Adsorption by Functionalized Nanoporous Materials: A Review. j nanosci nanotech. 2014 Feb 1;14(2):1811–22. <DOI>.

18. Yan B, Yu S, Zeng C, Yu L, Wang C, Zhang L. Binderless zeolite NaX microspheres with enhanced CO2 adsorption selectivity. Microporous and Mesoporous Materials. 2019 Apr;278:267–74. <DOI>.

19. Huang J, Zou J, Ho WSW. Carbon Dioxide Capture Using a CO_2 -Selective Facilitated Transport Membrane. Ind Eng Chem Res. 2008 Feb 1;47(4):1261–7. <DOI>.

20. Heyl D, Rodemerck U, Bentrup U. Mechanistic Study of Low-Temperature CO_2 Hydrogenation over Modified Rh/Al_2O_3 Catalysts. ACS Catal. 2016 Sep 2;6(9):6275–84. <DOI>.

21. Liu J, An T, Li G, Bao N, Sheng G, Fu J. Preparation and characterization of highly active mesoporous TiO2 photocatalysts by hydrothermal synthesis under weak acid conditions. Microporous and Mesoporous Materials. 2009 Aug;124(1–3):197–203. <DOI>.

22. Hiyoshi N, Yogo K, Yashima T. Adsorption characteristics of carbon dioxide on organically functionalized SBA-15. Microporous and Mesoporous Materials. 2005 Sep;84(1–3):357–65. <DOI>.

23. Zhou Y, Lu J, Zhou Y, Liu Y. Recent advances for dyes removal using novel adsorbents: A review. Environmental Pollution. 2019 Sep;252:352–65. <DOI>.

24. Lv Y, Xin Z, Meng X, Tao M, Bian Z, Gu J, et al. Essential role of organic additives in preparation of efficient Ni/KIT-6 catalysts for CO methanation. Applied Catalysis A: General. 2018 May;558:99–108. <DOI>.

25. Wei Y, Cai W, Deng S, Li Z, Yu H, Zhang S, et al. Efficient syngas production via dry reforming of renewable ethanol over Ni/KIT-6 nanocatalysts. Renewable Energy. 2020 Jan;145:1507–16. <DOI>.

26. Ouyang H, Guo L, Li C, Chen X, Jiang B. Fabrication and adsorption performance for CO2 capture of advanced nanoporous microspheres enriched with amino acids. Journal of Colloid and Interface Science. 2018 Dec;532:433–40. <DOI>.

27. Loganathan S, Ghoshal AK. Amine tethered pore-expanded MCM-41: A promising adsorbent for CO 2 capture. Chemical Engineering Journal. 2017 Jan;308:827–39. <DOI>.

28. Cecilia JA, Vilarrasa-García E, García-Sancho C, Saboya RMA, Azevedo DCS, Cavalcante CL, et al. Functionalization of hollow silica microspheres by impregnation or grafted of amine groups for the CO 2 capture. International Journal of Greenhouse Gas Control. 2016 Sep;52:344–56. <DOI>.

29. Wang W, Qi R, Shan W, Wang X, Jia Q, Zhao J, et al. Synthesis of KIT-6 type mesoporous silicas with tunable pore sizes, wall thickness and particle sizes via the partitioned cooperative self-assembly process. Microporous and Mesoporous Materials. 2014 Aug;194:167–73. <DOI>.

30. Mello MR, Phanon D, Silveira GQ, Llewellyn PL, Ronconi CM. Amine-modified MCM-41 mesoporous silica for carbon dioxide capture. Microporous and Mesoporous Materials. 2011 Aug;143(1):174–9. <DOI>.

31. Wang L, Ma L, Wang A, Liu Q, Zhang T. CO2 Adsorption on SBA-15 Modified by Aminosilane. Chinese Journal of Catalysis. 2007 Sep;28(9):805–10. <DOI>.

32. Hu Y, Liu W, Sun J, Yang X, Zhou Z, Zhang Y, et al. High Temperature CO_2 Capture on Novel Yb_2O_3 -Supported CaO-Based Sorbents. Energy Fuels. 2016 Aug 18;30(8):6606–13. <DOI>.

33. Chi C, Li Y, Ma X, Duan L. CO2 capture performance of CaO modified with by-product of biodiesel at calcium looping conditions. Chemical Engineering Journal. 2017 Oct;326:378–88. <DOI>.